

Hydrodynamic stimulation of dinoflagellate bioluminescence: a computational and experimental study

Michael I. Latz^{1,*}, Andrew R. Juhl^{1,†}, Abdel M. Ahmed², Said E. Elghobashi² and Jim Rohr^{1,3}

¹*Scripps Institution of Oceanography, University of California San Diego, 9500 Gilman Drive, La Jolla, CA 92093-0202, USA*, ²*Mechanical and Aerospace Engineering Department, University of California, Irvine, CA 92697, USA* and ³*SSC San Diego, 53560 Hull Street, D363, San Diego, CA 92152, USA*

*Author for correspondence (e-mail: mlatz@ucsd.edu)

†Present address: US EPA, ORD, NHEERL, Gulf Ecology Division, 1 Sabine Island Drive, Gulf Breeze, FL 32561, USA

Accepted 11 March 2004

Summary

Dinoflagellate bioluminescence provides a near-instantaneous reporter of cell response to flow. Although both fluid shear stress and acceleration are thought to be stimulatory, previous studies have used flow fields dominated by shear. In the present study, computational and experimental approaches were used to assess the relative contributions to bioluminescence stimulation of shear stress and acceleration in a laminar converging nozzle. This flow field is characterized by separate regions of pronounced acceleration away from the walls, and shear along the wall. Bioluminescence of the dinoflagellates *Lingulodinium polyedrum* and *Ceratocorys horrida*, chosen because of their previously characterized different flow sensitivities, was imaged with a low-light video system. Numerical simulations were used to calculate the position of stimulated cells and the levels of acceleration and shear stress at these positions. Cells were stimulated at the nozzle throat within the wall boundary

layer where, for that downstream position, shear stress was relatively high and acceleration relatively low. Cells of *C. horrida* were always stimulated significantly higher in the flow field than cells of *L. polyedrum* and at lower flow rates, consistent with their greater flow sensitivity. For both species, shear stress levels at the position of stimulated cells were similar to but slightly greater than previously determined response thresholds using independent flow fields. *L. polyedrum* did not respond in conditions where acceleration was as high as 20 g. These results indicate that shear stress, rather than acceleration, was the stimulatory component of flow. Thus, even in conditions of high acceleration, dinoflagellate bioluminescence is an effective marker of shear stress.

Key words: acceleration, bioluminescence, *Ceratocorys*, dinoflagellate, flow, *Lingulodinium*, numerical simulation, shear.

Introduction

Fluid motion affects the morphology, growth, physiology, feeding, reproduction, bioluminescence and behavior of planktonic organisms (e.g. Latz et al., 1994; Peters and Marrasé, 2000; Zirbel et al., 2000). Different responses to flow may be elicited by different hydrodynamic stimuli, although the basis for all known forms of mechanoreception is thought to involve physical deformation of cellular components. Some behavioral responses of planktonic organisms appear to be associated with fluid acceleration, suggesting that cell deformation or mechanoreceptor activation occurs due to extension along streamlines in the accelerating flow. For example, the escape reactions of copepods and ciliates have been associated with acceleration (Yen and Fields, 1992; Fields and Yen, 1996, 1997; Kiørboe et al., 1999; Jakobsen, 2001; Titelman, 2001). On the other hand, some responses to fluid motion are associated with tangential shear stress (hereafter, shear stress), due to velocity gradients across streamlines that presumably cause cell deformation. One

example is the effect of shear on population growth of dinoflagellates (Thomas and Gibson, 1990, 1992; Juhl et al., 2000, 2001; Juhl and Latz, 2002).

Flow-stimulated dinoflagellate luminescence is well known anecdotally from numerous observations of oceanic bioluminescence associated with breaking surface waves, swimming organisms and moving ships (e.g. Hobson, 1966; Staples, 1966; Tett and Kelley, 1973; Rohr et al., 1998). Ecologically, dinoflagellate bioluminescence is thought to serve an anti-predatory role (Esaias and Curl, 1972; White, 1979; Buskey et al., 1983, 1985; Mensinger and Case, 1992; Fleisher and Case, 1995). Laboratory studies of dinoflagellate bioluminescence indicate that fluid shear stress is an important stimulatory component (Latz et al., 1994; Latz and Rohr, 1999), although fluid acceleration has also been suggested as a stimulus for bioluminescence (Anderson et al., 1988). The objective of this study was to examine the response of luminescent dinoflagellates in an independent flow field that

allowed assessment of the relative stimulatory contributions of acceleration and shear stress. In this context, acceleration was associated with velocity gradients along a streamline and not unsteady or angular velocity.

The present study used a smooth converging nozzle, providing a laminar flow field, to assess the importance of shear stress and acceleration in stimulating dinoflagellate bioluminescence. Advantages of this flow field are: (1) regions of relatively high shear stress and acceleration are spatially separated, (2) properties of the flow field change continually along the downstream direction and (3) the governing hydrodynamic equations are exactly known. Moreover, compared with previous flow fields used to study bioluminescence stimulation (Latz et al., 1994; Latz and Rohr, 1999), the nozzle flow is unique in that there is no depletion of bioluminescence capacity prior to measurement.

Laboratory tests were performed over a range of flow rates for two dinoflagellate species, *Lingulodinium polyedrum* (formerly *Gonyaulax polyedra*) and *Ceratocorys horrida*. *L. polyedrum*, approximately 35 µm in diameter and common in coastal waters (Lewis and Hallett, 1997), is the most well-characterized dinoflagellate in terms of its luminescent response to flow (e.g. Anderson et al., 1988; Latz et al., 1994; Latz and Rohr, 1999). The oceanic species *C. horrida*, endemic to warm oligotrophic regions (Graham, 1942), is approximately twice as large as *L. polyedrum* and possesses prominent antapical spines (Zirbel et al., 2000). Both species have similar flash durations of approximately 150 ms (Latz and Lee, 1995), resulting in a pathline illuminating the cell trajectory in the flow (Latz et al., 1995). Previous studies with fully developed pipe flow indicate that the threshold luminescent response of *C. horrida* occurs in flows with shear stress levels approximately one order of magnitude less than for *L. polyedrum* (Nauen, 1998).

The following hypotheses were tested:

(1) Bioluminescence will occur in regions of high shear stress. In nozzle flow, high shear stress is present only in the nozzle throat near the wall. If acceleration stimulates bioluminescence, flashes will occur outside the wall boundary layer where fluid acceleration is highest.

(2) At equivalent flow rates, cells of *C. horrida* will respond further upstream than *L. polyedrum*, in regions where shear stresses are less.

The position of cell stimulation and the corresponding flow properties at those locations were determined using a combination of video observations of individual flashes within the nozzle and numerical simulations of the flow field for identical flow conditions as the experiments.

Materials and methods

The flow apparatus consisted of a 119 cm-long × 22 cm-wide × 13 cm-deep head tank connected to a converging nozzle test section and an exit pipe, all fabricated of clear acrylic. The convergence tapered from a 2.54 cm inlet diameter to an exit diameter of 0.32 cm, giving a contraction ratio of 8:1. The

contraction was axisymmetric along the centerline and can be described as:

$$Y(X) = \frac{1}{2}(Y_{in} - Y_e) \cos(\pi X/L) + \frac{1}{2}(Y_{in} + Y_e), \quad (1)$$

where $Y(X)$ is the radius at position X along the length ($L=6.4$ cm) of the contraction; Y_{in} is the radius at the inlet ($Y_{in}=1.27$ cm) where $X=0$, Y_e is the radius at the nozzle exit ($Y_e=0.16$ cm) where $X=L$, and π is in radians. The test section, subsequently referred to as the nozzle, included a 0.9 cm entrance length with radius Y_{in} and 1.1 cm exit length with radius Y_e . The narrowest section of the nozzle (the bottom third) is referred to as the throat. An exit pipe with the same radius as the nozzle exit delivered the effluent to a catch reservoir.

Flow from the head tank through the nozzle was driven by gravity and controlled by a manual valve at the pipe exit. The Reynolds number (Re) of each flow rate ($Re=\rho U_{avg}D/\mu$, where ρ is fluid density and μ is fluid dynamic viscosity) was calculated based on average flow velocity (U_{avg}) at the nozzle exit diameter D (where $D=2Y_e$), determined from measurements of volumetric flow rate made at the beginning, end and at 1-min intervals throughout each experiment. Values of Re were rounded off to the nearest hundred. Observations of injected dye confirmed that the flow remained laminar for all flow rates tested.

Experimental approach

Cultures of *Lingulodinium polyedrum* Stein Dodge and *Ceratocorys horrida* Stein were grown in half-strength f/2 medium (Guillard and Ryther, 1962) minus silicate and maintained at $20\pm 0.5^\circ\text{C}$ in an environmental chamber on a 12 h:12 h light:dark cycle as previously described (Latz and Rohr, 1999).

Two types of experiments were performed. Cell suspension experiments, in which a homogenous distribution of organisms was present in the flow field, involved no *a priori* assumptions about the position of cell stimulation. Cell injection experiments introduced cells at specific radial positions at the nozzle inlet to verify the position of stimulated cells as determined by the cell suspension experiments.

Prior to the end of the light phase, when cells are mechanically inexcitable (Biggley et al., 1969; Latz and Lee, 1995), subsamples of the cultures were diluted with 0.45 µm filtered seawater if necessary and, depending on the experiment, added to the head tank for cell suspension experiments or loaded into syringes for cell injection experiments. At the beginning of the dark phase, the room was darkened and cells were thereafter subjected to short periods of dim red light only. Testing commenced 2.5–4 h into the dark phase, when stimulated bioluminescence is maximal (Biggley et al., 1969; Latz and Lee, 1995). Room temperature was 19–20°C and varied by <0.5°C during each experiment.

Bioluminescence within the nozzle was imaged with an intensified SIT video camera (Cohu Inc. model 55) or intensified CCD video camera (Dage GenIISYS), each fitted with a Fujinon 25 mm lens used at f/0.85 or f/1.4 and fitted

with a +4 diopter lens. Video frame rate was 30 Hz. The 12 cm-wide camera field of view encompassed the entire nozzle, with the focal plane centered on the nozzle centerline.

For cell suspension experiments, cultures of either *L. polyedrum* or *C. horrida* were diluted into filtered seawater to give a final volume of 16 liters and a calculated cell concentration of 15 or 30 cells ml⁻¹, respectively. Random swimming by both species helped maintain a nearly homogenous distribution of organisms; thus, it was assumed that mean cell concentration did not vary within a test. A single daily experiment consisted of one filling of the head tank and tests with several flow rates.

Cell injection experiments examined the response of cells introduced at known radial positions at the nozzle inlet. Cells were injected at the nozzle inlet along a radius in a plane perpendicular to the axis of the camera. Cells were loaded into 60 ml plastic syringes fitted to Teflon™ tubing coupled to a plastic pipette tip with a 0.04 cm orifice. The tip orifice was positioned flush with the inlet of the nozzle, with the radial position of the tip controlled by a micromanipulator. Cells were injected at the nozzle inlet at a rate of 0.008 ml s⁻¹. Dye studies were first performed using the identical injection apparatus to visualize the trajectory of injected material at different radial positions. The dye stream was observed to remain in the injection plane throughout its passage through the nozzle, confirming that the radial position of injected material could be measured directly from the two-dimensional video record.

Two types of cell injection experiments were performed. First, using *L. polyedrum*, a series of eight radial positions between wall and centerline was tested at $Re \approx 2500$ (Table 1). Second, cells of *L. polyedrum* and *C. horrida* were injected at centerline to verify that, because of their response latency, they were not responding out of view of the initial camera position. This concern is greatest for cells moving along centerline, where flow velocity is highest and cells stimulated within the nozzle could respond as much as several centimeters downstream of the nozzle. To verify that cells were not being stimulated downstream out of the camera view, the camera position was moved so that it imaged 20 cm downstream of the nozzle to account for a response latency as high as 0.1 s, five times the estimated response latency of 20 ms (Widder and Case, 1981). Cells were injected at centerline for the highest flow rate tested in the cell suspension experiments. Periodically, the injector position was moved to the wall to verify cell stimulability.

Video analysis

The objective of the video analysis of cell suspension and injection experiments was to provide the position of each flash response so that subsequent numerical simulations could calculate the position of cell stimulation and the hydrodynamic parameters at that location. Although *L. polyedrum* and *C. horrida* can produce more than one flash (Latz and Lee, 1995), during the brief residence time in the nozzle no more than 1 flash cell⁻¹ was observed. Flashes typically lasted for 3–4

Table 1. Description of experimental conditions

Condition	Reynolds number	Inlet injection position
<i>L. polyedrum</i>		
Uniform	800, 2500, 5100	–
Injected	2500	0.1 cm increments from wall
Injected	5100	Wall, centerline only
<i>C. horrida</i>		
Uniform	400, 900, 2300, 5100	–
Injected	5100	Wall, centerline only
Dye		
Injected	2500	Wall, centerline only

successive video frames and, because the cells were moving, appeared as streaks within each video frame (Fig. 1). Approximately 40 individual flashes were analyzed for each flow rate using single-frame playback of the video record on a video monitor. The precision for measuring the position of a flash on the screen of the video monitor was 0.05 cm. Unless otherwise stated, values represent the arithmetic mean with one standard error of the mean. In some cases, median values were used for comparison between flow rates. Statistical tests were performed using Statview software (SAS Institute, Inc., Cary, NC, USA).

The downstream position, X_1 , of flash initiation was always obtained directly from the individual video frames. For cell injection experiments, the radial position of flash initiation, Y_1 , was also measured directly from the video record because flashes occurred in the injection plane normal to the camera. For cell suspension experiments, flash radial position could not be measured directly because flashes could occur azimuthally at any angle within the nozzle; therefore, a different analysis method was required. For this case, the flash radial position, Y_1 , was estimated from average flash velocity, determined by the change in position of the leading edge of a flash streak in consecutive video frames. Given X_1 and flash velocity, Y_1 was calculated from the numerical flow simulations. For both types of experiments, once the downstream and radial positions of flash initiation (X_1 , Y_1) were determined, numerical simulations adjusted for flash latency to provide the position of cell stimulation (X_0 and Y_0) and the values of acceleration and shear stress at that position (see next section).

As a check for accuracy, both methods of determining radial position, Y_1 , were compared for a subset of flashes recorded during the cell injection experiments. As previously described, for injected cells the radial position of flash initiation can be determined directly from each video frame by direct measurement. These radial positions were compared with those estimated from the average flash speed analysis using numerical simulations.

Numerical simulations

Numerical simulations of the nozzle flow field allowed for high-resolution mapping of the position of organism

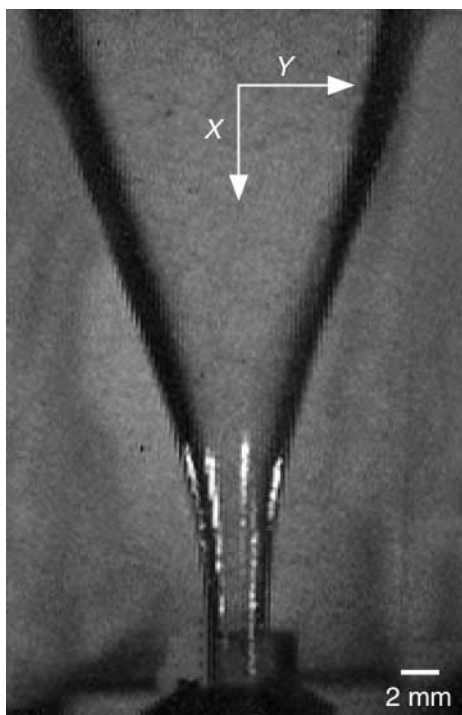


Fig. 1. Imaging of luminescent response of cells of *Lingulodinium polyedrum* for $Re=5100$. A composite of several video frames shows responses for five cells superimposed on a view of the nozzle. Each streak represents the trajectory of a single flash response.

stimulation and the flow parameters at that position. This approach was especially important because flow properties changed continuously in the downstream direction. Numerical simulations served three purposes: (1) to obtain the radial position of flash initiation, Y_1 , for cell suspension experiments; (2) to account for the response latency of organisms within the developing flow field, such that the position of cell stimulation was upstream of that for flash initiation; and (3) to calculate values of acceleration and shear stress at the position of stimulated cells.

For these simulations, it was assumed that the organisms behaved as fluid particles and that their presence had no effect on the flow. This assumption is quite plausible because the volume fraction of the organisms, approximately 10^{-7} , was

sufficiently low (Elghobashi, 1994), their density is only slightly greater than that of the liquid water (Kamykowski et al., 1992) so they are almost neutrally buoyant, and their local swimming speed (Kamykowski et al., 1992) is much less than the carrier flow velocity. Previous pipe flow experiments at these organism concentrations demonstrated no effect on the Newtonian nature of the flow (Latz and Rohr, 1999). Moreover, video recordings of flash and dye trajectories from cell and dye injection studies showed no apparent differences, suggesting that, for the purpose of calculating the position of stimulation, individual cells followed fluid streamlines.

The numerical method computed the properties (velocity and pressure) of the flow inside the nozzle. This flow was laminar, incompressible and axisymmetric. The governing equations were the Navier–Stokes and continuity equations, which are expressions of conservation of momentum and mass, respectively. These partial differential equations were discretized on a boundary-fitted orthogonal curvilinear grid generated by solving a system of Laplace equations with suitable boundary conditions to satisfy orthogonality. Prescribed boundary conditions were: no-slip along the nozzle wall, axisymmetry along centerline, uniform velocity profile at the nozzle inlet plane, and zero axial velocity at the exit plane.

For the two-dimensional nozzle geometry, there were two coordinate variables, X and Y . The geometry was mapped from the physical domain X, Y onto a uniformly spaced orthogonal ξ, η domain (Mobley and Stewart, 1980). The resulting grid allowed the governing equations to be discretized using the finite volume method in which the solution domain was divided into contiguous quadrilateral curvilinear control volumes. A modified SIMPLE algorithm (Patankar, 1980) was used to solve the discretized equations and obtain the two components of velocity and pressure at the grid nodes.

The following steps were taken to obtain the flow conditions responsible for stimulation of the organism (Table 2). The flow field was computed for similar Reynolds numbers as the experiments. The downstream (X_1) and radial (Y_1) position of flash initiation was obtained as described in the previous section. The final position (X_0 and Y_0) of organism stimulation was calculated from X_1 and Y_1 by following the streamline upstream an additional 20 ms to account for the response latency (Widder and Case, 1981). The hydrodynamic properties at the stimulation position (X_0 and Y_0) were

Table 2. Parameters of flow used in numerical simulations

Symbol (units)	Parameter
X_0 (m)	Downstream position of cell stimulation; calculated by numerical simulation
Y_0 (m)	Radial position of cell stimulation; calculated by numerical simulation
X_1 (m)	Downstream position of flash initiation; measured from the video record
Y_1 (m)	Radial position of flash initiation; for cell injection experiments measured from the video record, calculated by numerical simulations for cell suspension experiments
Re	Reynolds number; proportional to flow rate and nozzle diameter
U_{avg} ($m\ s^{-1}$)	Average flow velocity at the nozzle exit

See Materials and methods for details.

calculated using cubic-spline interpolation of the properties at the fixed grid nodes.

The effect of steady and changing pressure on bioluminescence stimulation was not considered in this study because dinoflagellates are known to be relatively insensitive to pressure (Gooch and Vidaver, 1980; Swift et al., 1981; Krasnow et al., 1981; Donaldson et al., 1983). If shear stress thresholds of 0.1 N m^{-2} for luminescent dinoflagellates were the same for pressure, above-threshold levels would exist essentially throughout the entire ocean (Rohr et al., 2002).

Results

Computational description of the nozzle flow field

Velocity vectors derived from the computational simulation showed that the velocity profile was approximately flat, except near the walls. The region of flow where the velocity was less than 10% that of centerline (referred to as the wall boundary layer) was a convenient demarcation indicating where cross-stream velocity gradients (proportional to shear stress) were relatively large. Velocity gradients along streamlines (proportional to acceleration) were greatest away from the nozzle walls and at the nozzle throat (Fig. 2). Maximum acceleration achieved during this study was 200 m s^{-2} along centerline at $X=5.75 \text{ cm}$ for $Re=5100$. For all flows tested, shear stress was negligible outside the wall boundary layer and zero along centerline. The shear stress contour of 0.1 N m^{-2} , approximating the response threshold for *L. polyedrum* (Latz et al., 1994; Latz and Rohr, 1999), was always located within the boundary layer. For the range of flow rates used in this study, the maximum thickness of the flow field with shear stress levels of $>0.1 \text{ N m}^{-1}$ was $0.04\text{--}0.05 \text{ cm}$. The shear stress contour of 0.02 N m^{-2} , representing the shear stress response threshold of *C. horrida* (Nauen, 1998), was also contained within the boundary layer; the maximum thickness of the layer with shear stress levels of $>0.02 \text{ N m}^{-1}$ was $0.07\text{--}0.14 \text{ cm}$.

Cell suspension experiments

Despite being distributed throughout the flow volume, flash responses of *L. polyedrum* and *C. horrida* were only observed at the nozzle throat (Fig. 1). For both species, the downstream position, X_1 , of flash initiation (Fig. 3) shifted significantly upstream with increasing flow rate (one-way ANOVA: *L. polyedrum*, $F=313.1$, $d.f.=2, 119$, $P<0.0001$; *C. horrida*, $F=136.5$, $d.f.=3, 160$, $P<0.0001$). The differences between species were consistent with the higher flow sensitivity of *C. horrida* (Nauen, 1998). First, the minimum flow rate to which *C. horrida* responded ($Re=400$) was lower than for *L. polyedrum* ($Re=800$). Second, at similar flow rates, flashes of *C. horrida* were initiated higher in the nozzle than for *L. polyedrum*. For example, at the highest flow rate tested ($Re=5100$) the mean downstream position of $3.9\pm 0.08 \text{ cm}$ for *C. horrida* was significantly different from that of $4.8\pm 0.03 \text{ cm}$ for *L. polyedrum* (t -test, $t=9.94$, $d.f.=81$, $P<0.0001$).

Greater than 99% of all cells were stimulated within the boundary layer; four responses by *L. polyedrum* attributed to

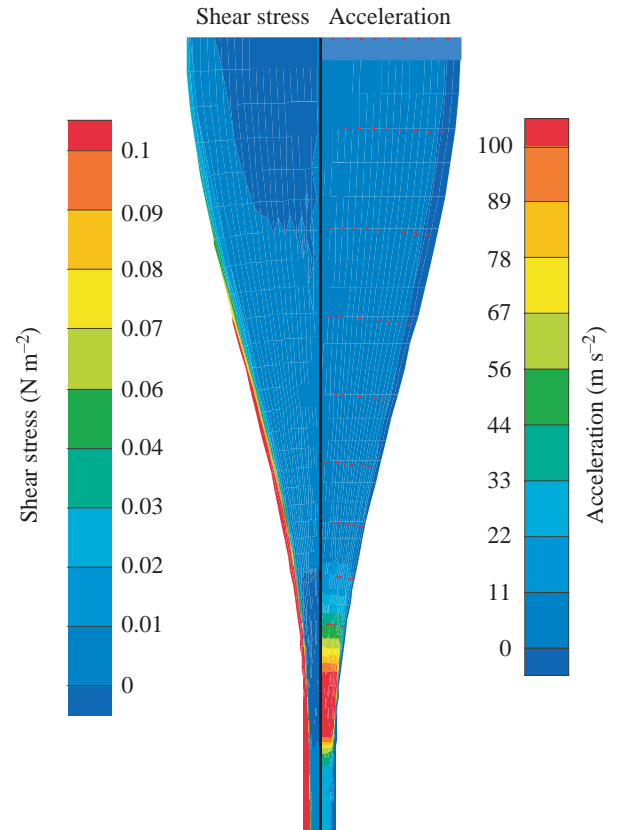


Fig. 2. Map of the nozzle flow field for numerical simulations at $Re=5100$ showing color contours of fluid shear stress (left half) and acceleration (right half).

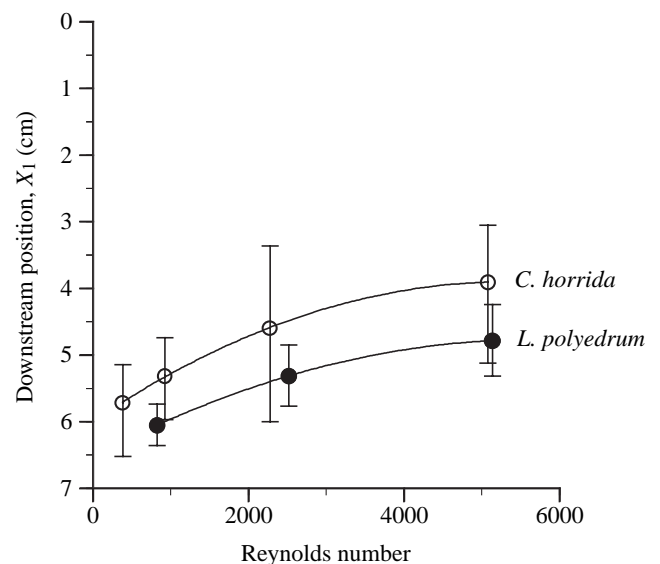


Fig. 3. Downstream position of flash initiation (X_1) by *Lingulodinium polyedrum* (filled symbols) and *Ceratocorys horrida* (open symbols) as a function of Reynolds number of the flow. Symbols represent median values with minimum and maximum range for approximately 40 cells at each flow. *C. horrida* responded at lower flow rates, and flashes were typically located further upstream than for *L. polyedrum*.

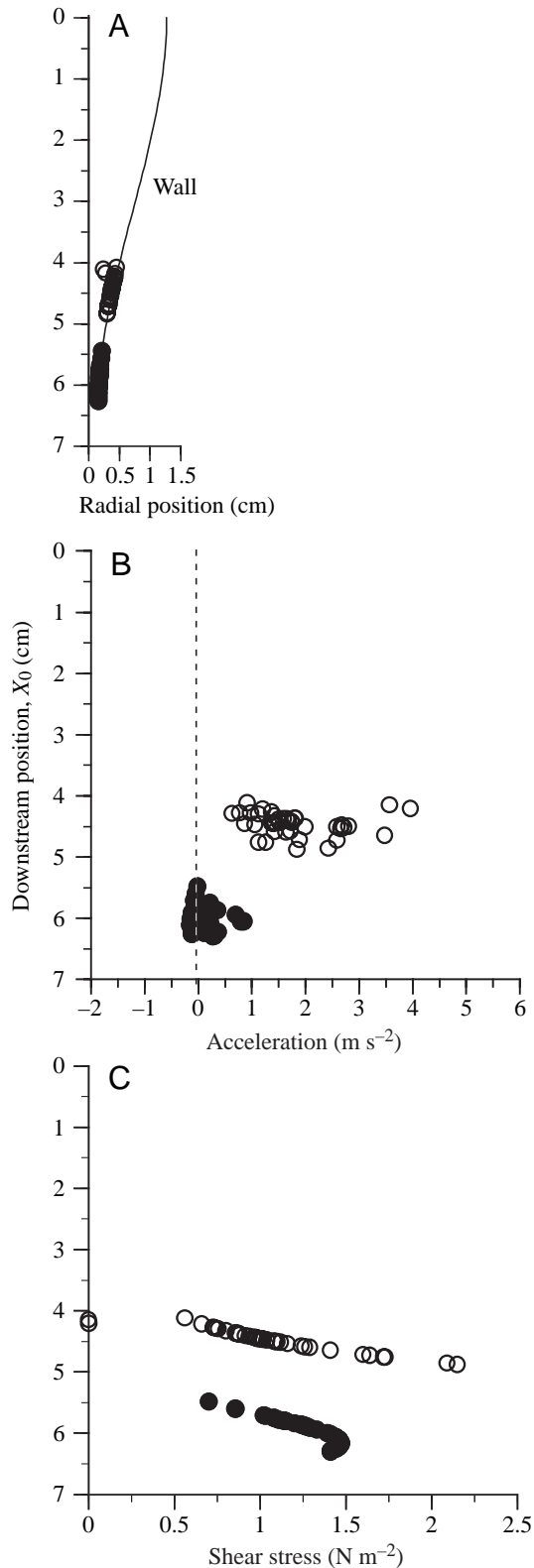


Fig. 4. Flow conditions, based on numerical simulations, at the position (X_0 , Y_0) of stimulated cells of *Lingulodinium polyedrum* for cell suspension experiments. Each point represents the results for a single cell; approximately 40 cells were analyzed for each flow rate. Filled symbols are for $Re=800$ while open symbols are for $Re=5100$. (A) Position of stimulated cells. Curved line represents the position of the wall. (B) Fluid acceleration. The broken line represents a value of zero acceleration. (C) Fluid shear stress.

within the boundary layer (data not shown). Values of acceleration at the position of stimulated cells were always $<4 \text{ m s}^{-2}$ and frequently near zero, especially at the lowest flow rate (Fig. 4). The minimum value of shear stress at these cell positions within the boundary layer was 0.7, 0.6 and 0.6 N m^{-2} for $Re=800$, 2500 and 5100, respectively.

All *C. horrida* cells were stimulated within the boundary layer, with a mean of $<0.028 \text{ cm}$ from the wall (data not shown). At $Re=400$, the minimum stimulatory flow rate tested, values of fluid acceleration at the position of stimulated cells were $<0.59 \text{ m s}^{-2}$ ($<0.1 \text{ g}$) (Fig. 5). At these positions, shear stress was $0.08\text{--}0.44 \text{ N m}^{-2}$. Even at the highest flow rate tested ($Re=5100$), all stimulated cells were located near the wall where acceleration was $<2 \text{ m s}^{-2}$ ($\sim 0.2 \text{ g}$). The minimum value of shear stress at the cell positions was 0.08, 0.17, 0.05 and 0.09 N m^{-2} for $Re=400$, 900, 2300 and 5100, respectively.

To assess the relative stimulatory effects of acceleration and shear stress, values at the position of stimulated cells (X_0 , Y_0) were normalized to maximum levels along the nozzle radius, Y , for that downstream X_0 position. For both species, mean values of shear stress were 79–100% of maximum when mean values of acceleration were only 3–21% of maximum (Fig. 6).

Calculation of the position of a stimulated cell is sensitive to the value of response latency used in the numerical simulations. For example, a longer response latency will translate the position of stimulation further upstream from the position of flash initiation. Because the response latency of *L. polyedrum* and *C. horrida* to flow stimulation is unknown, the value of 20 ms, obtained for mechanical stimulation of the dinoflagellate *Pyrocystis fusiformis* (Widder and Case, 1981), was used. To examine the sensitivity of the computational results to the chosen value of response latency, differences in the calculated position of stimulated cells of *L. polyedrum* as a function of response latency were assessed for three flow rates. Latency values of 5, 10, 15 and 25 ms were tested in addition to the 20 ms standard. At the lowest flow rate tested ($Re=800$), there were no resolvable differences in downstream cell position and the ranges of acceleration and shear stress at the position of stimulated cells for the different latency values. At the intermediate flow rate of $Re=2500$, increasing latency values ‘pushed’ the position of stimulated cells further upstream, resulting in decreases in values of shear stress at the cell position but resulting in minimal differences in acceleration. At the highest flow rate ($Re=5100$), the value of response latency affected both the cell downstream position and shear stress at the position of stimulated cells. However,

cells outside the boundary layer may have been spontaneous flashes (Sweeney and Hastings, 1958; Latz and Lee, 1995) and not flow stimulated. For all flow rates, *L. polyedrum* cells were stimulated at a mean position of $<0.035 \text{ cm}$ from the wall,

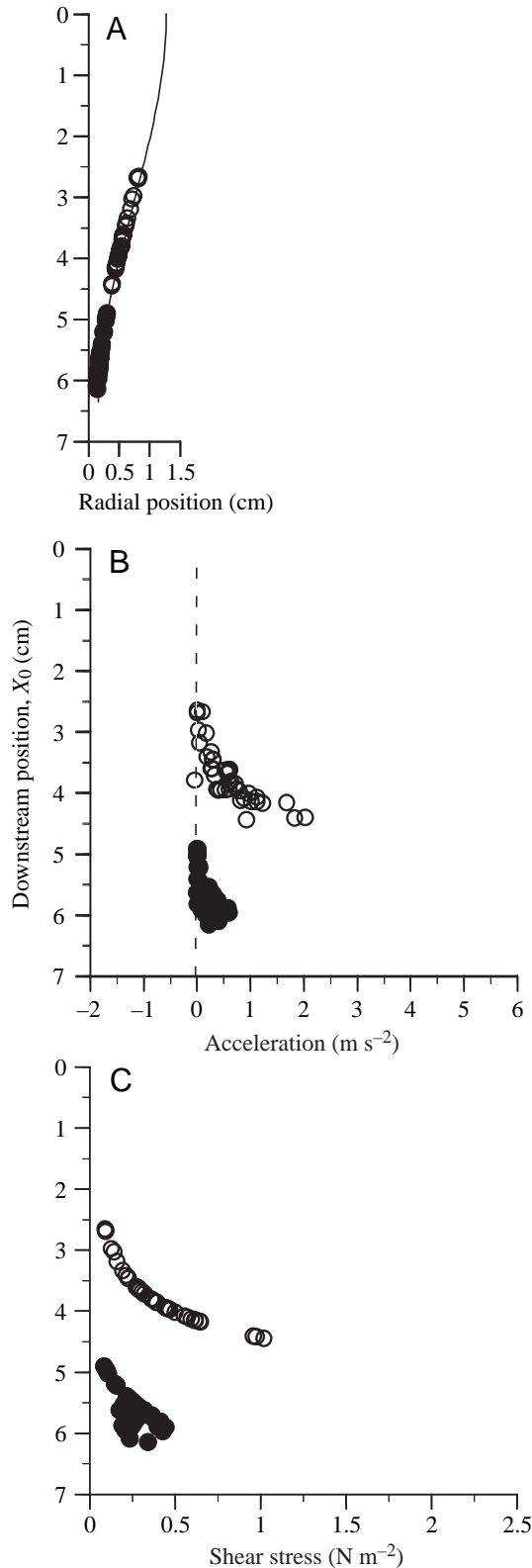


Fig. 5. Flow conditions, based on numerical simulations, at the position (X_0, Y_0) of stimulated cells of *Ceratocorys horrida* for cell suspension experiments. Filled symbols are for $Re=400$ while open symbols are for $Re=5100$. (A) Position of stimulated cells. Curved line represents the position of the wall. (B) Fluid acceleration. The broken line represents a value of zero acceleration. (C) Fluid shear stress.

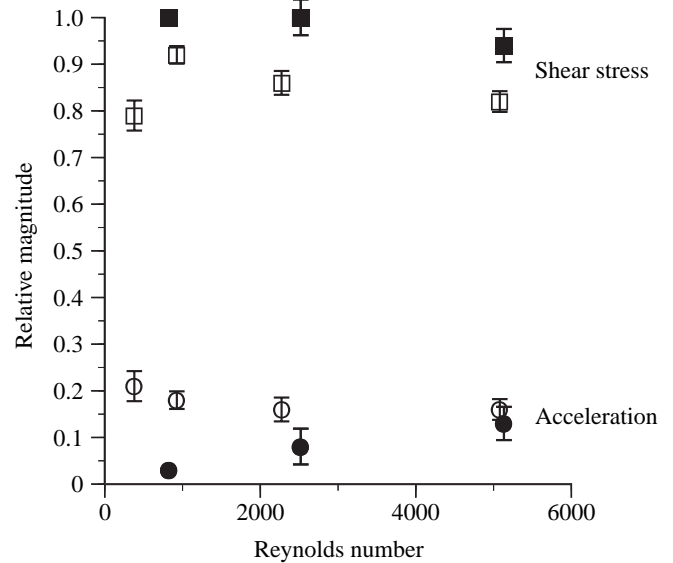


Fig. 6. Relative fluid shear stress and acceleration at the position (X_0, Y_0) of stimulated cells of *Lingulodinium polyedrum* (closed symbols) and *Ceratocorys horrida* (open symbols). Relative values were calculated as the ratio of the flow parameter at the position of a stimulated cell to the maximum value of that parameter for any Y at that downstream (X_0) position in the flow field. Boxes and circles are for relative shear stress and acceleration, respectively. Values represent means \pm S.E.M. for approximately 40 cells at each flow condition.

regardless of the chosen value of response latency, cells were always stimulated in the boundary layer where shear stress levels were high compared with elsewhere in the flow field.

Cell injection experiments

To further confirm that organisms were stimulated within the wall shear layer and not in the region of high acceleration, cells of *L. polyedrum* were injected at the nozzle inlet in the plane normal to the axis of the camera at different radial positions from centerline to the inlet wall. No flashes were observed at the injector, suggesting that there was minimal pre-stimulation of cells due to the injection procedure. Only cells injected at $>0.7Y_{in}$ were stimulated within the nozzle (Fig. 7A). Stimulated cells had a mean downstream position, X_0 , of 5.5 cm and were located approximately 0.01 cm from the wall, within the boundary layer (data not shown). The maximum response rate of 71% of injected cells, for an injection position of $0.8Y_{in}$, indicated that most cells were responding. Shear stress levels at the position of stimulated cells were near maximum for that downstream (X) position, while acceleration was $<10\%$ of maximum levels outside the boundary layer (Fig. 7B).

Cell injection experiments also allowed comparison of the numerical simulation estimates of Y_0 with those from direct video analysis. Analysis of 40 flashes, from an experiment in which cells were injected at $0.8Y_{in}$ at the nozzle inlet at $Re=2500$, showed little difference between the two methods.

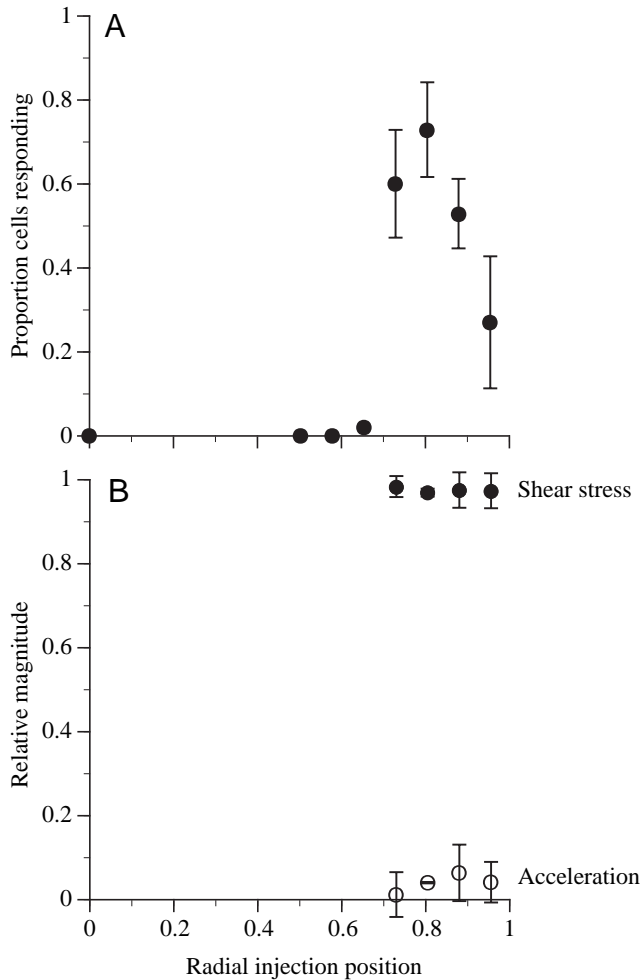


Fig. 7. Response of cells of *Lingulodinium polyedrum* injected at the nozzle inlet at various radial positions for $Re=2500$. A radial injection position of 1 is at the inlet wall ($=Y_{in}$) while a value of zero is at centerline. Symbols represent mean values \pm S.D. (A) Proportion of cells responding, based on approximately 7 cells injected s^{-1} ; cells injected at $<0.6Y_{in}$ did not respond. All stimulated cells were located downstream within the thin wall boundary layer. (B) Relative fluid shear stress and acceleration at the position of stimulated cells (X_0 , Y_0).

Video analysis gave a radial position $Y_1=0.23\pm 0.03$ cm at a downstream position $X_1=5.31\pm 0.19$ cm; the numerical simulations calculated a radial position $Y_0=0.22\pm 0.02$ cm at $X_0=5.46\pm 0.18$ cm. The difference between methods was less than the uncertainty associated with determining the flash initiation position on the video monitor. Although each method has its own assumptions and limitations, both predict flash positions within the boundary layer and yield similar response trends.

Because centerline velocities were as high as 2 m s^{-1} , a response latency of 20 ms could result in flashes occurring as much as 4 cm downstream from where they were stimulated, possibly outside the initial camera field of view. To account for this possible bias, cells injected along centerline were

monitored up to 20 cm downstream of the nozzle exit. Dye experiments showed that the flow remained laminar throughout this region. At $Re=5100$, the highest flow rate tested in this study, no flashes from >3000 cells of *L. polyedrum* injected at centerline were observed either within the nozzle or downstream of the nozzle within the exit pipe. For almost 3000 cells of *C. horrida* injected at centerline for $Re=5100$, 3% of the cells were observed responding within the exit pipe. During these experiments, cell viability was confirmed by periodically moving the injection point to the inlet wall, where numerous flashes were observed.

Discussion

The nozzle flow field provided spatial separation of regions of high acceleration, outside the boundary layer, from those of high shear stress within the thin boundary layer at the nozzle throat. This flow pattern was similar for all flow rates and allowed for unambiguous assessment of the stimulatory component of flow. For both dinoflagellate species tested, whether cells were in suspension or injected, flashes were stimulated near the wall in the nozzle throat. In this region shear stress levels were relatively high compared with elsewhere in the flow field, whereas levels of acceleration were relatively low. Flashes were rarely stimulated outside the boundary layer even though levels of acceleration were as high as 20 g . Based on the spatial pattern of stimulation, it is concluded that cell stimulation was due to fluid shear stress and not acceleration. If cells had been responding to acceleration, then flashes would have been expected outside the boundary layer where levels of acceleration were much greater. Injection of *L. polyedrum* cells at centerline demonstrated they were not responding to acceleration downstream beyond the field of view of the camera. Therefore, even in a highly accelerating flow field, the luminescent response of *L. polyedrum* was associated with shear stress.

Changes in flow rate affected the levels of acceleration and shear stress within the flow field but did not alter the general flow pattern. For both species, there was a significant change in the downstream position of stimulated cells, as the stimulation position moved upstream with increasing flow rate. This response was consistent with the higher levels of shear stress within the upstream boundary layer as flow rate increased. A comparison of the responses of the two species indicated that differences in the spatial pattern of stimulation reflected the species flow sensitivity. *C. horrida* stimulated cells were positioned higher in the flow field, for equivalent flow rates, and responded at lower flow rates than for *L. polyedrum*, consistent with the former's greater flow sensitivity (Nauen, 1998).

For three completely independent flow fields – simple Couette flow, fully developed pipe flow and nozzle flow – the luminescent response is consistent with a mechanism of stimulation based on fluid shear. These first two flow fields are dominated by shear. For Couette flow in the gap between concentric cylinders, with the outer cylinder rotating, there is

a nearly linear velocity gradient (and thus nearly constant shear) between the outer and inner cylinders; the mean shear stress in the gap changes as a function of angular rotation (van Duuren, 1968). Although there is centripetal acceleration, there is no acceleration along velocity gradients. In fully developed laminar pipe flow, the parabolic velocity distribution across the pipe radius results in a gradient of shear stress, with maximum shear at the wall and zero shear at centerline (Schlichting, 1979). In this flow field there is no mean acceleration and the mean shear profile across the pipe is balanced by the pressure gradient. In nozzle flow, used in the present study, most of the volume is dominated by acceleration, with only a thin shear layer near the wall at the nozzle throat. Nozzle flow is also different from the other flow fields in that it presents a developing flow field where flow parameters change dramatically throughout the volume.

For all three flow fields, response thresholds are determined based on the minimum flow condition in which bioluminescence is stimulated. In the present study with nozzle flow, a response threshold was obtained for each flow rate based on the minimum shear stress value at the position of all stimulated cells. For *L. polyedrum*, the response threshold for shear stress was 0.6 N m^{-2} . This response threshold is similar to, although somewhat higher than, the shear stress threshold of 0.3 N m^{-2} obtained for fully developed pipe flow at similar concentrations (Latz and Rohr, 1999). For *C. horrida*, the shear stress response threshold obtained for nozzle flow was 0.05 N m^{-2} while that for fully developed pipe flow is 0.02 N m^{-2} (Nauen, 1998). Considering that a difference in flash location of as small as 0.01 cm can result in significantly different flow properties, as well as the uncertainty in organism response latency, the experimental results using nozzle flow were remarkably consistent with those from other flow fields. Overall, these results demonstrate that organisms are responding to specific, quantitative, hydrodynamic aspects of the flow, regardless of the flow field used.

Flow sensing

Dinoflagellate bioluminescence is considered to have an anti-predator function by decreasing grazing pressure (Esaias and Curl, 1972; White, 1979) through altering predator swimming behavior (Buskey et al., 1983, 1985). However, the response threshold for dinoflagellate bioluminescence, occurring in flows with shear stress levels in the order of 0.1 N m^{-2} (Latz et al., 1994; Nauen, 1998; Latz and Rohr, 1999; present study), equivalent to fluid strain rates of approximately 100 s^{-1} , is several orders of magnitude higher than response thresholds for flow-stimulated predator avoidance behaviors by other planktonic organisms (reviewed by Kjørboe et al., 1999; Jakobsen, 2001). Are levels of fluid strain sufficient to stimulate bioluminescence present in the feeding current of a predator? Using siphon flow as a mimic of a grazer feeding current, a feeding current flow rate of 0.279 ml s^{-1} (table 2 of Jakobsen, 2001) and equation 2 of

Kjørboe et al. (1999), bioluminescence stimulation is estimated to occur at a distance of only 0.06 cm from the siphon inlet. If the siphon flow field represents the feeding current of a filtering dinoflagellate predator, then dinoflagellate bioluminescence would only be stimulated very close to the predator. Video observations of the interactions between dinoflagellates and their copepod grazers verify that bioluminescence is associated with feeding activities and not flow disturbance (Buskey et al., 1985). Therefore, it is unlikely that dinoflagellate bioluminescence is stimulated by the flow within a predator feeding current, as are the escape behaviors of copepods, rotifers and ciliates. Rather, stimulation may occur either by direct handling of the cell by a grazer or by the shear stress produced by a moving organism. Bioluminescence generated by swimming animals in a 'minefield' of luminescent dinoflagellates can allow visual predators to better find prey (Mensing and Case, 1992; Fleisher and Case, 1995). Oceanic conditions providing supra-threshold shear levels include not only the boundaries of swimming organisms (Rohr et al., 1998) but also flow at the ocean boundaries and in highly turbulent events such as breaking waves (Rohr et al., 2002).

Under what conditions would accelerating flows be stimulatory? In a study of *L. polyedrum* (Anderson et al., 1988), bioluminescence was not stimulated by steady centripetal acceleration as high as 100 g or changing centripetal acceleration of 1 g s^{-1} . Only variable centripetal acceleration of the order of 10 g s^{-1} , associated with abrupt starts and stops of a rotating chamber, were considered stimulatory, but it is unclear if the stimulation resulted from the acceleration change or from vibration or start/stop transients. In the present study, accelerations as high as 20 g , with estimated rates of change of $>10 \text{ g s}^{-1}$, were not stimulatory to *L. polyedrum*. It is unlikely that accelerations above this magnitude are prevalent in the ocean, so acceleration is not an ecologically relevant stimulus of dinoflagellate bioluminescence.

Nevertheless, highly accelerating flows may be important tools in understanding mechanotransduction. Flow stimuli are believed to elicit bioluminescence as a result of cell deformation, leading to a signaling process involving a calcium-mediated second messenger pathway (von Dassow and Latz, 2002). The initial step may involve changes in membrane fluidity (Mallipattu et al., 2002) or activation of plasma membrane proteins as in other flow-sensitive organisms (Gudi et al., 1996; Labrador et al., 2003). This process leads to generation of an action potential at the vacuole membrane (Eckert, 1966) that results in proton flux into the cytoplasm, activating the luminescent chemistry (Fritz et al., 1990). Flow conditions with equivalent levels of fluid strain are expected to cause identical amounts of cell deformation, whether the strain is due to elongation within an accelerating fluid (due to the velocity gradient along a streamline) or shear (due to the velocity gradient across streamlines). Bioluminescence should therefore be stimulated in highly accelerating flows in which the elongation stress is greater than

the known threshold for shear stress. The equivalence of elongation and shear in eliciting a biological response was experimentally validated for escape swimming of the copepod *Acartia tonsa* (Kiørboe et al., 1999). The issue is difficult to investigate for bioluminescence stimulation because of the very high flow rates necessary to obtain sufficiently high levels of fluid strain from acceleration.

Dinoflagellate flow visualization

Dinoflagellate bioluminescence is a powerful tool for flow visualization under conditions not amenable to conventional methods (Latz et al., 1995; Rohr et al., 1998). Organisms are the size of typical flow markers (Irani and Callis, 1973), can remain in suspension due to cell swimming or near-neutral buoyancy, respond nearly instantaneously within regions of above threshold shear stress, and can be used at cell concentrations that have no effect on the Newtonian nature of the fluid. A further advantage is that dinoflagellate bioluminescence is easily visualized and quantified. Unlike visualization of conventional flow markers, bioluminescence can be detected by low-light camera systems at distances in the order of meters, without the need to optically discriminate individual organisms. The level of average bioluminescence intensity, a function of species abundance, stimulatory volume and level, and the number of organisms responding (Rohr et al., 1998; Latz and Rohr, 1999), is readily measured by extremely sensitive photomultiplier detectors. Demonstrated uses of dinoflagellate flow visualization include visualization of boundaries and flow separation (Latz et al., 1995; Rohr et al., 1998) and pinpointing regions of high shear in bioreactors (Chen et al., 2003). Possible applications of luminescent flow visualization include mapping regions of high shear in prosthetic heart valve flows (Yoganathan et al., 1998) and identifying highly dissipative regions of flow in the ocean (Rohr et al., 2002).

The present study successfully incorporated computational and experimental fluid approaches to examine a transient biological process. Even though the organisms were advected through this flow field of the order of seconds, the near-instantaneous luminescent response and use of numerical simulations allowed high-resolution mapping of the stimulatory regions of the flow field. Computational approaches have tremendous potential in determining the forces on, and deformation of, small organisms in both laminar and turbulent flows (e.g. Jiang et al., 2002). When coupled with numerical simulations, the experimental use of dinoflagellate bioluminescence is an effective technique to resolve flow properties at the small spatial and temporal scales relevant to the organism and holds promise for providing new understanding of complex flow phenomena (Stokes et al., 2004).

We are grateful to J. Nauen for technical assistance and initial discussions. Supported by the Office of Naval Research (grant N00014-95-1-0001 to M.I.L.) and ILIR/IAR programs at SSC San Diego (to J.R.).

References

- Anderson, D. M., Nosenchuck, D. M., Reynolds, G. T. and Walton, A. J. (1988). Mechanical stimulation of bioluminescence in the dinoflagellate *Gonyaulax polyedra* Stein. *J. Exp. Mar. Biol. Ecol.* **122**, 277-288.
- Biggley, W. H., Swift, E., Buchanan, R. J. and Seliger, H. H. (1969). Stimulable and spontaneous bioluminescence in the marine dinoflagellates, *Pyrodinium bahamense*, *Gonyaulax polyedra*, and *Pyrocystis lunula*. *J. Gen. Physiol.* **54**, 96-122.
- Buskey, E., Mills, L. and Swift, E. (1983). The effects of dinoflagellate bioluminescence on the swimming behavior of a marine copepod. *Limnol. Oceanogr.* **28**, 575-579.
- Buskey, E. J., Reynolds, G. T., Swift, E. and Walton, A. J. (1985). Interactions between copepods and bioluminescent dinoflagellates: direct observations using image intensification. *Biol. Bull.* **169**, 530.
- Chen, A. K., Latz, M. I. and Frangos, J. A. (2003). The use of bioluminescence to characterize cell stimulation in bioreactors. *Biotechnol. Bioeng.* **83**, 93-103.
- Donaldson, T. Q., Tucker, S. P. and Lynch, R. V. (1983). Stimulation of bioluminescence in dinoflagellates by controlled pressure changes. *Naval Res. Lab. Report* **8772**.
- Eckert, R. (1966). Excitation and luminescence in *Noctiluca miliaris*. In *Bioluminescence in Progress* (ed. F. Johnson and Y. Haneda), pp. 269-300. Princeton, NJ: Princeton University Press.
- Elghobashi, S. E. (1994). On predicting particle-laden turbulent flows. *Appl. Sci. Res.* **52**, 309-329.
- Esaias, W. E. and Curl, H. C., Jr (1972). Effect of dinoflagellate bioluminescence on copepod ingestion rates. *Limnol. Oceanogr.* **17**, 901-906.
- Fields, D. M. and Yen, J. (1996). The escape behavior of *Pleuromamma xiphias* in response to a quantifiable fluid mechanical disturbance. *Mar. Freshw. Behav. Physiol.* **27**, 323-340.
- Fields, D. M. and Yen, J. (1997). Implications of the feeding current structure of *Euchaeta rimana*, a carnivorous pelagic copepod, on the spatial orientation of their prey. *J. Plankton Res.* **19**, 79-95.
- Fleisher, K. J. and Case, J. F. (1995). Cephalopod predation facilitated by dinoflagellate luminescence. *Biol. Bull.* **189**, 263-271.
- Fritz, L., Morse, D. and Hastings, J. W. (1990). The circadian bioluminescence rhythm of *Gonyaulax* is related to daily variations in the number of light-emitting organelles. *J. Cell Sci.* **95**, 321-328.
- Gooch, V. D. and Vidaver, W. (1980). Kinetic analysis of the influence of hydrostatic pressure on bioluminescence of *Gonyaulax polyedra*. *Photochem. Photobiol.* **31**, 397-402.
- Graham, H. W. (1942). Studies in the morphology, taxonomy, and ecology of the Peridinales. *Scient. Results Cruise VII Carnegie, Biol. Ser.* **3**, 1-129.
- Gudi, S. R. P., Clark, C. B. and Frangos, J. A. (1996). Fluid flow rapidly activates G proteins in human endothelial cells. Involvement of G proteins in mechanochemical signal transduction. *Circ. Res.* **79**, 834-839.
- Guillard, R. R. L. and Ryther, J. H. (1962). Studies of marine planktonic diatoms. I. *Cyclotella nana* Husted, and *Detonula confervacea* (Cleve) Gran. *Can. J. Microbiol.* **8**, 229-239.
- Hobson, E. S. (1966). Visual orientation and feeding in seals and sea lions. *Nature* **214**, 326-327.
- Irani, R. R. and Callis, C. F. (1973). *Particle Size: Measurement, Interpretation, and Application*. New York: Wiley.
- Jakobsen, H. H. (2001). Escape response of planktonic protists to fluid mechanical signals. *Mar. Ecol. Progr. Ser.* **214**, 67-78.
- Jiang, H., Meneveau, C. and Osborn, T. R. (2002). The flow field around a freely swimming copepod in steady motion. Part II: Numerical simulation. *J. Plankton Res.* **24**, 191-213.
- Juhl, A. R. and Latz, M. I. (2002). Mechanisms of fluid shear-induced inhibition of population growth of a red-tide dinoflagellate. *J. Phycol.* **38**, 683-694.
- Juhl, A. R., Velazquez, V. and Latz, M. I. (2000). Effect of growth conditions on flow-induced inhibition of population growth of a red-tide dinoflagellate. *Limnol. Oceanogr.* **45**, 905-915.
- Juhl, A. R., Trainer, V. L. and Latz, M. I. (2001). Effect of fluid shear and irradiance on population growth and cellular toxin content of the dinoflagellate *Alexandrium fundyense*. *Limnol. Oceanogr.* **46**, 758-764.
- Kamykowski, D., Reed, R. E. and Kirkpatrick, G. J. (1992). Comparison of sinking velocity, swimming velocity, rotation and path characteristics among six marine dinoflagellate species. *Mar. Biol.* **113**, 319-328.
- Kiørboe, T., Saiz, E. and Visser, A. (1999). Hydrodynamic signal perception in the copepod *Acartia tonsa*. *Mar. Ecol. Progr. Ser.* **179**, 97-111.
- Krasnow, R., Dunlap, J., Taylor, W., Hastings, J. W., Vetterling, W. and

- Haas, E.** (1981). Measurements of *Gonyaulax* bioluminescence including that of single cells. In *Bioluminescence Current Perspectives* (ed. K. H. Nealson), pp. 52-63. Minneapolis: Burgess Publishing.
- Labrador, V., Chen, K.-D., Li, Y.-S., Muller, S., Stoltz, J.-F. and Chien, S.** (2003). Interactions of mechanotransduction pathways. *Biorheology* **40**, 47-52.
- Latz, M. I. and Lee, A. O.** (1995). Spontaneous and stimulated bioluminescence in the dinoflagellate, *Ceratocorys horrida* (Peridinales). *J. Phycol.* **31**, 120-132.
- Latz, M. I. and Rohr, J.** (1999). Luminescent response of the red tide dinoflagellate *Lingulodinium polyedrum* to laminar and turbulent flow. *Limnol. Oceanogr.* **44**, 1423-1435.
- Latz, M. I., Case, J. F. and Gran, R. L.** (1994). Excitation of bioluminescence by laminar fluid shear associated with simple Couette flow. *Limnol. Oceanogr.* **39**, 1424-1439.
- Latz, M. I., Rohr, J. and Hoyt, J.** (1995). A novel flow visualization technique using bioluminescent marine plankton – Part I: Laboratory studies. *IEEE J. Oceanic Eng.* **20**, 144-147.
- Lewis, J. and Hallett, R.** (1997). *Lingulodinium polyedrum* (*Gonyaulax polyedra*) a blooming dinoflagellate. *Oceanogr. Mar. Biol. Annu. Rev.* **35**, 97-161.
- Mallipattu, S. K., Haidekker, M. A., von Dassow, P., Latz, M. I. and Frangos, J. A.** (2002). Evidence for shear-induced increase in membrane fluidity in the dinoflagellate *Lingulodinium polyedrum*. *J. Comp. Physiol. A* **188**, 409-416.
- Mensingher, A. F. and Case, J. F.** (1992). Dinoflagellate luminescence increases susceptibility of zooplankton to teleost predation. *Mar. Biol.* **112**, 207-210.
- Mobley, C. D. and Stewart, R. J.** (1980). Numerical generation of boundary-fitted orthogonal curvilinear coordinate systems. *J. Comput. Phys.* **34**, 124-135.
- Nauen, J. C.** (1998). Biomechanics of two aquatic defense systems. *Ph.D. Dissertation*. University of California, San Diego.
- Patankar, S. V.** (1980). *Numerical Heat Transfer and Fluid Flow*. Washington: Hemisphere Pub. Corp.; New York: McGraw-Hill.
- Peters, F. and Marrasé, C.** (2000). Effects of turbulence on plankton: an overview of experimental evidence and some theoretical considerations. *Mar. Ecol. Prog. Ser.* **205**, 291-306.
- Rohr, J., Latz, M. I., Fallon, S., Nauen, J. C. and Hendricks, E.** (1998). Experimental approaches towards interpreting dolphin-stimulated bioluminescence. *J. Exp. Biol.* **201**, 1447-1460.
- Rohr, J., Hyman, M., Fallon, S. and Latz, M. I.** (2002). Bioluminescence flow visualization in the ocean: an initial strategy based on laboratory experiments. *Deep-Sea Res. I* **49**, 2009-2033.
- Schlichting, H.** (1979). *Boundary-Layer Theory*. New York: McGraw-Hill.
- Staples, R. F.** (1966). The distribution and characteristics of surface bioluminescence in the oceans. *Naval Oceanographic Office Technical Report No. 184*.
- Stokes, M. D., Deane, G. B., Rohr, J. and Latz, M. I.** (2004). Bioluminescence imaging of wave-induced turbulence. *J. Geophys. Res.* **109**, C01004.
- Sweeney, B. M. and Hastings, J. W.** (1958). Rhythmic cell division in populations of *Gonyaulax polyedra*. *J. Protozool.* **5**, 217-224.
- Swift, E. Meunier, V. A., Biggley, W. H., Hoarau, J. and Barras, H.** (1981). Factors affecting bioluminescent capacity in oceanic dinoflagellates. In *Bioluminescence Current Perspectives* (ed. K. H. Nealson), pp. 95-106. Minneapolis, MN: Burgess Publishing Co.
- Tett, P. B. and Kelley, M. G.** (1973). Marine bioluminescence. *Oceanogr. Mar. Biol. A. Rev.* **11**, 89-173.
- Thomas, W. H. and Gibson, C. H.** (1990). Quantified small-scale turbulence inhibits a red tide dinoflagellate, *Gonyaulax polyedra* Stein. *Deep-Sea Res.* **37**, 1583-1593.
- Thomas, W. H. and Gibson, C. H.** (1992). Effects of quantified small-scale turbulence on the dinoflagellate *Gymnodinium sanguineum* (*splendens*): contrasts with *Gonyaulax* (*Lingulodinium*) *polyedra*, and the fishery implication. *Deep-Sea Res.* **39**, 1429-1437.
- Titelman, J.** (2001). Swimming and escape behavior of copepod nauplii: implications for predator-prey interactions among copepods. *Mar. Ecol. Prog. Ser.* **213**, 203-213.
- van Duuren, F. A.** (1968). Defined velocity gradient model flocculator. *J. Sanitary Eng. Div.* **94**, 671-682.
- von Dassow, P. and Latz, M. I.** (2002). The role of Ca²⁺ in stimulated bioluminescence of the dinoflagellate *Lingulodinium polyedrum*. *J. Exp. Biol.* **205**, 2971-2986.
- White, H. H.** (1979). Effects of dinoflagellate bioluminescence on the ingestion rates of herbivorous zooplankton. *J. Exp. Mar. Biol. Ecol.* **36**, 217-224.
- Widder, E. A. and Case, J. F.** (1981). Bioluminescence excitation in a dinoflagellate. In *Bioluminescence Current Perspectives* (ed. K. H. Nealson), pp. 125-132. Minneapolis, MN: Burgess Publishing Co.
- Yen, J. and Fields, D. M.** (1992). Escape responses of *Acartia hudsonica* (Copepoda) nauplii from the flow field of *Temora longicornis* (Copepoda). *Ergebnisse Limnol.* **36**, 123-134.
- Yoganathan, A. P., Ellis, J. T., Healy, T. M. and Chatzimavroudis, G. P.** (1998). Fluid dynamic studies for the year 2000. *J. Heart Valve Disease* **7**, 130-139.
- Zirbel, M. J., Veron, F. and Latz, M. I.** (2000). The reversible effect of flow on the morphology of *Ceratocorys horrida* (Peridinales, Dinophyta). *J. Phycol.* **36**, 46-58.